RESEARCH ARTICLE

Characteristics of inorganic phosphorus fractions and their correlations with soil properties in three non-acidic soils

ZHANG Nai-yu[1], WANG Qiong[1, 2], ZHAN Xiao-ying[3], WU Qi-hua[4], HUANG Shao-min[5], ZHU Ping[6], YANG Xue-yun[7], ZHANG Shu-xiang[1]

[1] *Institute of Agricultural Resources and Regional Planning, Chinese Academy of Agricultural Sciences/National Engineering Laboratory for Improving Quality of Arable Land, Beijing 100081, P.R.China*

[2] *TERRA, Gembloux Agro-Bio Tech, University of Liege, Gembloux 5030, Belgium*

[3] *Institute of Environment and Sustainable Development in Agriculture, Chinese Academy of Agricultural Sciences, Beijing 100081, P.R.China*

[4] *Institute of Bioengineering, Guangdong Academy of Sciences/Guangdong Modern Agricultural Technology Research and Development Center, Guangzhou 510316, P.R.China*

[5] *Institute of Plant Nutrient, Agricultural Resources and Environmental Sciences, Henan Academy of Agricultural Sciences, Zhengzhou 450002, P.R.China*

[6] *Institute of Agricultural Resources and Environment, Jilin Academy of Agricultural Sciences, Changchun 130033, P.R.China*

[7] *College of Natural Resources and Environment, Northwest A&F University, Yangling 712100, P.R.China*

Abstract

Understanding the characteristics and influences of various factors on phosphorus (P) fractions is of significance for promoting the efficiency of soil P. Based on long-term experiments on black soil, fluvo-aquic soil, and loess soil, which belong to Phaeozems, Cambisols, and Anthrosols in the World Reference Base for Soil Resources (WRB), respectively, five fertilization practices were selected and divided into three groups: no P fertilizer (CK/NK), balanced fertilizer (NPK/NPKS), and manure plus mineral fertilizer (NPKM). Soil inorganic P (Pi) fractions and soil properties were analyzed to investigate the characteristics of the Pi fractions and the relationships between Pi fractions and various soil properties. The results showed that the proportion of Ca_{10}-P in the sum of total Pi fractions was the highest in the three soils, accounting for 33.5% in black soil, 48.8% in fluvo-aquic soil, and 44.8% in loess soil. Long-term fertilization practices resulted in periodic changes in soil Pi accumulation or depletion. For black soil and fluvo-aquic soil, the Pi accumulation was higher in the late period (10–20 years) of fertilization than in the early period (0–10 years) under NPK/NPKS and NPKM, whereas the opposite result was found in loess soil. The Pi accumulation occurred in all Pi fractions in black soil; mainly in Ca_8-P, Fe-P, and Ca_{10}-P in fluvo-aquic soil; and in Ca_2-P, Ca_8-P, and O-P in loess soil. Under CK/NK, the soil Pi was depleted mainly in the early period in each of the three soils. In addition to the labile Pi (Ca_2-P) and moderately

labile Pi (Ca_8-P, Fe-P, Al-P), the Ca_{10}-P in black soil and fluvo-aquic soil and O-P in loess soil could also be used by crops. Redundancy analysis showed that soil properties explained more than 90% of the variation in the Pi fractions in each soil, and the explanatory percentages of soil organic matter (SOM) were 43.6% in black soil, 74.6% in fluvo-aquic, and 38.2% in loess soil. Consequently, decisions regarding the application of P fertilizer should consider the accumulation rate and the variations in Pi fractions driven by soil properties in non-acidic soils.

Keywords: non-acidic soils, long-term fertilization, phosphorus fractions, soil properties, organic matter

1. Introduction

During the past half-century, the input of phosphorus (P) fertilizer in cropland has been increasing to meet the food demands associated with population growth (Chen and Graedel 2016; Jiao *et al.* 2016). Due to the adsorption, precipitation, and microbial immobilization of P in the soil, most of the P applied as fertilizer cannot be used by plants directly (Yadav and Verma 2012; Weihrauch and Opp 2018; Zhu *et al.* 2018), resulting in massive P surpluses in many regions (MacDonald *et al.* 2011). Commercially, P is mainly derived from P rock resources, which will be depleted within 100 years at the current rate of production (Cooper *et al.* 2011). Thus, making full use of soil surplus P is important for solving the shortage of P resources and maintaining food security (Li H *et al.* 2011; De Oliveira *et al.* 2020).

Understanding the nature and dynamics of P in croplands is the key priority for fully utilizing soil P (Liu *et al.* 2017). P applications often lead to P surpluses in croplands, but the P forms vary with fertilization practices and soil types (Pizzeghello *et al.* 2011; Eriksson *et al.* 2015). For example, one study showed that superphosphate significantly decreased Ca_8-P in the calcareous soil in Iran (Khosravi *et al.* 2017). However, the opposite result was found in another calcareous soil in China (Liu *et al.* 2020). The content of Ca-P generally increased in soil treated with manure due to the existence of abundant Ca-P in manure, and the rate of increase depended not only on the amount of manure application, but also on the type of soil (Sato *et al.* 2005; Yamamoto *et al.* 2018; Yan *et al.* 2018). On the other hand, performing no applications of P can result in P depletion in croplands (De Oliveira *et al.* 2020), but soil P depletion varies with soil properties (Helfenstein *et al.* 2018). According to Helfenstein *et al.* (2018), some primary mineral P remains even after long-term soil development in arid-zone soils, whereas in humid-zone soils of the same age, all P in all of the pools has been biologically cycled in the natural ecosystem. P deficits provide an opportunity to understand the availability of P forms (Gatiboni *et al.* 2021). Although previous studies have revealed that the inorganic P (Pi) fraction variations are mainly affected by fertilization practices and soil types, most of those studies focused on a single soil type and few comparative studies on multiple soils at a regional scale have been reported.

Soil properties have shown an important effect on soil Pi fractions and transformations, and it is likely that each P compound has specific factors governing its presence (Deiss *et al.* 2018). For neutral soils or calcareous soils, calcium (Ca) ion is the main material for P adsorption (Hansen *et al.* 2004; Andersson *et al.* 2015), while iron (Fe) and aluminum (Al) hydroxides are also abundant and play important roles in the retention of P (Schmieder *et al.* 2018; Ma *et al.* 2021). Schmieder *et al.* (2018) reported that 76% of the soil P was associated with Al or Fe in long-term manure-amended soils under non-acidic conditions. Ma *et al.* (2021) observed a similar predominance of Fe minerals in P immobilization in chernozem soil. Generally, Ca, Fe, and Al cations or compounds have direct effects on P adsorption, resulting in the differences in soil Pi fractions (Weihrauch and Opp 2018). The P adsorption is usually indirectly affected by other properties such as soil organic matter (SOM) and pH (Fink *et al.* 2016; Meyer *et al.* 2021). SOM can promote P adsorption and availability mainly by cation bridges, increases in specific surface area (SSA), and competitive adsorption sites (Fink *et al.* 2016; Yang *et al.* 2019; Audette *et al.* 2020). Soil pH affects the process of P precipitation-dissolution reactions, in which decreases in pH increase solubilization of soil Al, increasing the precipitation of Al-P minerals (Meyer *et al.* 2021), and a significant decline in the soil pH can drive the solubilization of P held in Ca-P (Zhang *et al.* 2020). Therefore, the characteristics of soil Pi fractions depend on the comprehensive effect of many factors. So, comparative research of multiple soils is necessary to identify the main soil factors driving soil Pi fractions.

The black soil, fluvo-aquic soil, and loess soil areas are important grain production bases in North China, which play an important role in national food security. In this study, the three groups of no P fertilizer, balanced

fertilizer, and manure plus mineral fertilizer were used. We analyzed the Pi fractions and soil properties at three sites with different fertilizer application practices. These soils are all non-acidic and rich in Ca, so it is appropriate to analyze the Pi fractions by the method of Jiang and Gu (1989). Notably, the total P content was similar at about 0.6 g kg^{-1} at the beginning of the long-term experiments in the three soils, which provided an opportunity for investigating the characteristics and factors affecting the soil Pi fractions. The purposes of the study were to: 1) analyze the unique and common traits of Pi fractions in the three non-acidic soils under different fertilization practices, and 2) identify the soil properties driving the variations in Pi fractions, which can provide theoretical support for the efficient utilization of soil P in typical croplands across North China.

2. Materials and methods

2.1. Overview of study sites

The experiment was conducted at the Chinese National Soil Fertility and Fertilizer Efficiency Monitoring Base. The study sites of the three soils were located in Gongzhuling City, Jilin, Northeast China (124°48′E, 43°30′N, built in 1989), Zhengzhou City, Henan, Central China (113°40′E, 34°47′N, built in 1990), and Yangling City, Shaanxi, Northwest China (108°00′E, 34°17′N, built in 1990). The soil types in the Chinese Soil Taxonomy of Gongzhuling, Zhengzhou, and Yangling are black soil (Phaeozems, WRB), fluvo-aquic soil (Cambisol, WRB), and loess soil (Anthrosols, WRB), respectively. The climatic conditions and experimental management practices at each site have been described in previous studies (Wu *et al.* 2017; Khan *et al.* 2018; Shen *et al.* 2019). The total P contents of the initial surface soil (0–20 cm) at the three sites were each about 0.6 g kg^{-1}, but the other soil properties varied considerably among the three sites (Table 1).

2.2. Experimental design

In this study, five treatments were selected: (1) CK (no fertilizer control); (2) NK (nitrogen and potassium); (3) NPK (nitrogen, P and potassium); (4) NPKS (nitrogen,

P, potassium plus straw); and (5) NPKM (nitrogen, P, potassium plus farmyard manure). The annual fertilization rates are summarized in Table 2. Based on the P application rates, the five treatments were divided into three groups: no P fertilizer (CK/NK), balanced fertilizer (NPK/NPKS), and manure plus mineral fertilizer (NPKM). For historical reasons, the experimental design was not randomized, although it still provides valuable information for revealing the dynamic evolution of soil properties (Wang *et al.* 2021). Soils were obtained in different years due to the limited availability of the historical soil samples: Gongzhuling in 1990, 2000, and 2012; Zhengzhou in 1990, 2002, and 2012; and Yangling in 1990, 2000, and 2011. Three replications of each soil sample were collected for laboratory analysis, and the analysis results are expressed as the means of three replication samples.

2.3. Soil sampling and analyses

Soil samples were provided by the experiment stations and were collected after harvest every year and before fertilization. These samples from the arable layer (0–20 cm) were randomly collected at multiple points and were mixed, air-dried, sieved (2 mm), and stored. Partial soil samples were sieved (0.15 mm) again according to the analysis requirements.

SOM content was determined by vitriol acid-potassium dichromate oxidation (Lu 1999). Soil pH was determined by the potentiometric method (soil:water, 1:2.5) (Lu 1999). CaCO$_3$ was determined by volumetric titration (Lu 1999). Free Fe$_2$O$_3$ (DCB Fe) and free Al$_2$O$_3$ (DCB Al) were extracted by sodium dithionite-citrate-bicarbonate (DCB) at 80°C (Mehra and Jackson 1960). Mehlich-3-Fe, Al, Mg and Ca (M3-Fe, M3-Al, M3-Mg and M3-Ca) were extracted with the Mehlich-3 extraction reagent (Mehlich 1984). The metal materials extracted were analyzed for DCB Fe, DCB Al, M3-Fe, M3-Al, M3-Mg, and M3-Ca using inductively coupled plasma atomic emission spectroscopy (ICP-AES, Varian Inc., California, USA). Six soil Pi fractions were extracted using the sequential extraction method (Jiang and Gu 1989). Briefly, these Pi fractions were extracted serially with NaHCO$_3$ (Ca$_2$-P), NH$_4$AC (Ca$_8$-P), NH$_4$Cl+NH$_4$F

Table 1 Initial surface soil properties at the three experimental sites

Site	Soil type[1]	pH	SOM (g kg^{-1})[2]	Total N (g kg^{-1})	Total P (g kg^{-1})	Total K (g kg^{-1})	Olsen P (mg kg^{-1})
Gongzhuling	Black soil	7.6	22.8	1.40	0.61	18.42	11.79
Zhengzhou	Fluvo-aquic soil	8.3	12.2	0.64	0.69	16.90	6.50
Yangling	Loess soil	8.6	12.8	0.93	0.61	21.64	9.57

[1] Chinese Soil Taxonomy.
[2] SOM, soil organic matter.

Table 2 Annual fertilization rates (kg ha⁻¹) of N, P, and K for the different treatments at the three experimental sites

Site	Treatment[1]	N	P	K
Gongzhuling	CK	0	0	0
	NK	165	0	68
	NPK	165	36	68
	NPKS	112+53[2]	36+6[2]	68+58[2]
	NPKM	50+115[2]	36+39[2]	68+77[2]
Zhengzhou	CK	0	0	0
	NK	353	0	146
	NPK	353	77	146
	NPKS	309+44[2]	77+8[2]	146+86[2]
	NPKM	238+115[2]	77+66[2]	146+92[2]
Yangling	CK	0	0	0
	NK	353	0	147
	NPK	353	82	147
	NPKS	353+40[2]	82+4[2]	147+86[2]
	NPKM	237+115[2]	82+106[2]	147+139[2]

[1] CK, no fertilizer control; NK, nitrogen and potassium; NPK, nitrogen, P and potassium; NPKS, nitrogen, P, potassium plus straw; NPKM, nitrogen, P, potassium plus farmyard manure.
[2] The mean amounts of N/P/K contained in the added farmyard manure or straw.

(Al-P), $NaOH+Na_2CO_3$ (Fe-P), $Na_3Cit+Na_2S_2O_3+NaOH$ (O-P), and H_2SO_4 (Ca_{10}-P) extraction reagents. The Pi fractions are generally divided into labile P (Ca_2-P), moderately labile P (Ca_8-P, Al-P, and Fe-P), and stable P (O-P and Ca_{10}-P) categories. The P in the extracts was determined colorimetrically following the procedure of Murphy and Riley (1962). The stage change of P was taken as the difference in the P content between the

later years and previous years.

2.4. Statistical analyses

The differences of soil properties among the three soils were compared using SPSS 23 Software by ANOVA and the LSD test with a significance level at $P<0.05$. Canoco 5 Software was used for redundancy analysis (RDA) of the Pi fractions and soil properties. OriginPro 2021 Software was used to draw the figures.

3. Results

3.1. Pi fractions in three non-acidic soils

The distribution characteristics of the Pi fractions were different in the three non-acidic soils (Fig. 1-A–C). The highest proportion of the Pi fraction was Ca_{10}-P, which accounted for 33.5% in black soil, 48.8% in fluvo-aquic soil, and 44.8% in loess soil. Secondly, the proportion of O-P was 26% in black soil and 17.5% in fluvo-aquic soil. The proportion of moderately labile P (Ca_8-P, Al-P, and Fe-P) was 34.9% in black soil, 27.1% in fluvo-aquic soil, and 33.9% in loess soil. The proportion of labile P (Ca_2-P) was the lowest, and ranged from 5.6 to 6.7% in the three soils. It can be seen from the column heights of the boxplots in Fig. 1 that the smallest variation of the Pi fraction was O-P in black soil and fluvo-aquic
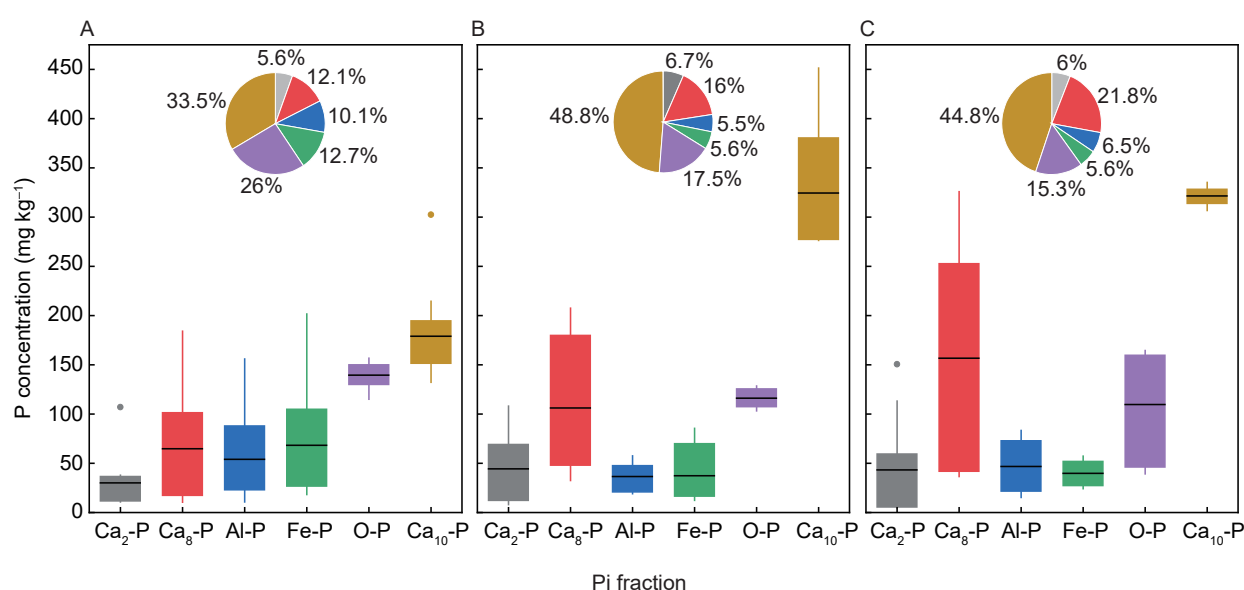

Fig. 1 Contents and proportions of Pi fractions in black soil (A), fluvo-aquic soil (B), and loess soil (C). The black lines in the boxplots indicate the mean values, and the lower and upper horizontal lines correspond to the first and third quartiles (i.e., the 25th and 75th percentiles). Data are shown from all the treatments at all the sampling times (n=11 for each Pi fraction). The upper and lower vertical lines in the boxplots indicate the largest and smallest values at 1.5IQR (where IQR is the interquartile range). The percentages in the pie charts indicate the proportions of each Pi fraction in the sum of total Pi fractions.

soil, whereas it was Ca_{10}-P in loess soil. Meanwhile, the largest variation of the Pi fraction was in Ca_8-P in all soils, suggesting that different fertilization practices mainly cause the variations in the Ca_8-P in non-acidic soils.

3.2. Changes in Pi fractions under different fertilization practices

The changes in soil Pi fractions were further compared under the different fertilization practices, as shown in Table 3. The total Pi of CK/NK in all soils decreased in the early stage (about 0–10 years). The total Pi decreased by 70.9 mg kg^{-1} in black soil (1990–2000), 45.3 mg kg^{-1} in fluvo-aquic soil (1990–2000), and 49 mg kg^{-1} in loess soil (1990–2000). This indicated that the Pi in black soil was more easily utilized. The decreases in the Pi fractions were mainly in the order of Ca_8-P>Fe-P≈Ca_{10}-P>Al-P in black soil, Ca_2-P>Ca_{10}-P in fluvo-aquic soil, and only O-P in loess soil, suggesting that these Pi fractions were potentially available P sources in the corresponding P-deficiency soils. O-P in black soil and fluvo-aquic soil and Ca_{10}-P in loess soil changed slightly in the early and late stages (about 10–20 years), indicating that they were difficult to utilize in the corresponding soils.

The accumulation of Pi in different Pi fractions was related to soil types and fertilization practices (Table 3). The Pi accumulation from the P fertilization applications (NPK/NPKS and NPKM) was concentrated in the late stage after 10 years of continuous fertilization in black soil and fluvo-aquic soil, whereas it was concentrated in the early stage in loess soil. For the late stage in black soil, the accumulation of Pi mainly occurred in Ca_8-P, Al-P, Fe-P, and O-P under NPK/NPKS, accounting for 78.82% of the total Pi accumulation, while the accumulation of Pi mainly occurred in Ca_2-P, Ca_8-P, Al-P, Fe-P, and Ca_{10}-P under NPKM, accounting for 80.98% of the total Pi accumulation. For the late stage in fluvo-aquic soil, the accumulation of Pi mainly occurred in the order of Ca_{10}-P, Ca_8-P, and Fe-P, accounting for 84.05% (NPK/NPKS) and 94.88% (NPKM) of the total Pi accumulation. For the early stage in loess soil, the accumulation of Pi mainly occurred in Ca_8-P and O-P under NPK/NPKS, accounting for 72.91% of the total Pi accumulation, whereas it mainly occurred in Ca_8-P and Ca_2-P under NPKM, accounting for 72.4% of the total Pi accumulation.

3.3. Properties of the three non-acidic soils

Soil properties varied greatly among the three non-acidic soils (Fig. 2-A–I). The contents of SOM, M3-Fe, M3-Al,

Table 3 Periodic changes (mg kg^{-1}) in the Pi fractions under different fertilization groups in each soil

Treatment[1]	Pi fraction	Black soil		Fluvo-aquic soil		Loess soil	
		1990–2000	2000–2012	1990–2002	2002–2012	1990–2000	2000–2011
CK/NK	Ca_2-P	−0.1	−4.0	−23.2	2.6	−2.8	0.4
	Ca_8-P	−28.5	−1.0	−4.3	−14.0	2.1	9.5
	Al-P	−11.4	−6.3	2.4	1.5	−9.7	1.5
	Fe-P	−21.9	−8.4	0.1	−2.3	−0.2	1.7
	O-P	12.5	9.0	−3.4	13.2	−48.4	6.8
	Ca_{10}-P	−21.5	−18.1	−16.9	2.6	10.0	2.5
	Total Pi	−70.9	−28.7	−45.3	3.4	−49.0	22.3
NPK/NPKS	Ca_2-P	8.6	19.1	4.5	25.7	34.0	7.5
	Ca_8-P	21.3	53.1	67.5	63.9	177.6	−16.5
	Al-P	7.4	40.3	26.0	3.6	32.8	−0.2
	Fe-P	8.0	43.1	14.5	42.1	15.2	11.0
	O-P	26.3	39.3	11.6	8.1	70.3	4.0
	Ca_{10}-P	−11.9	28.1	6.3	90.6	10.3	13.8
	Total Pi	59.6	222.9	130.3	233.9	340.0	19.7
NPKM	Ca_2-P	22.6	91.6	59.0	15.2	142.7	−37.6
	Ca_8-P	57.5	140.4	82.5	72.5	283.6	−10.4
	Al-P	53.4	121.3	24.7	13.2	47.5	6.8
	Fe-P	55.5	152.2	18.7	50.0	29.7	−7.9
	O-P	35.0	34.7	18.1	−15.2	63.1	3.9
	Ca_{10}-P	−7.3	126.0	35.6	122.0	21.6	7.1
	Total Pi	216.6	666.2	238.6	257.7	588.3	−38.2

[1] CK, no fertilizer control; NK, nitrogen and potassium; NPK, nitrogen, P and potassium; NPKS, nitrogen, P, potassium plus straw; NPKM, nitrogen, P, potassium plus farmyard manure.
Data are the difference of the Pi fraction contents between the late and early periods.

DCB Fe, and DCB Al in black soil were the highest, and the contents of M3-Ca and CaCO$_3$, and the pH value were the lowest, which were significantly (P<0.05) different from those in both fluvo-aquic soil and loess soil (Fig. 2-A–C, E–I). The contents of M3-Ca, M3-Mg, DCB Fe, DCB Al, and CaCO$_3$ were significantly (P<0.05) different between the fluvo-aquic soil and loess soil (Fig. 2-C and D, G–I).

3.4. Correlations between Pi fractions and soil properties

Redundancy analysis (RDA) was conducted to determine the correlations between Pi fractions and various soil properties (Fig. 3-A–D). The total variance of the Pi fractions explained by soil properties was 58.55% in the three soils (Fig. 3-A). DCB Al, SOM, and M3-Fe had significant (P<0.05) explanatory percentages, accounting for 29.4, 16.4, and 6%, respectively (Table 4). Soil properties explained more than 90% of the variations in Pi fractions of each soil (Fig. 3-B–D). For black soil, SOM and DCB Al had significant (P<0.05) explanatory percentages for the variations in Pi fractions, accounting for 43.6 and 27.1%, respectively. However, in fluvo-aquic soil the variation was mainly due to SOM and M3-Fe, accounting for 74.6 and 10%, and in loess soil SOM and M3-Ca were the main contributors, accounting for 38.2 and 11.3%, respectively (Table 4). These results indicated that soil properties, especially SOM, explained the variations in soil Pi fractions in non-acidic soils pretty well.
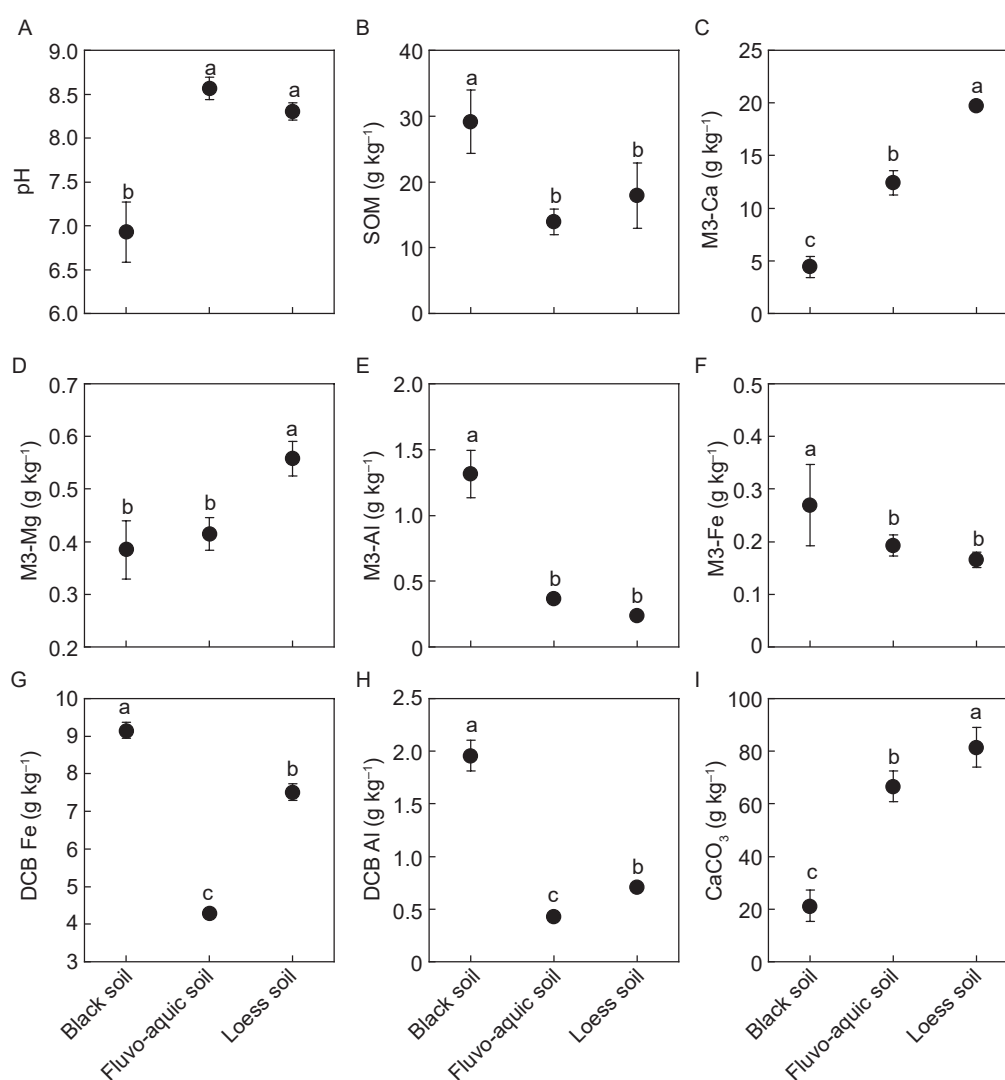

Fig. 2 Soil properties of the three non-acidic soils. SOM, soil organic matter; M3-Ca, M3-Mg, M3-Al, and M3-Fe, Mehlich-3 extraction reagent extracted Ca, Mg, Al, and Fe, respectively; DCB Fe, free Fe$_2$O$_3$; DCB Al, free Al$_2$O$_3$. Data are shown from all the treatments at all the sampling times (n=11). The circles indicate the mean values with the error bars of the first and third quartiles (the 25th and 75th percentiles). Different letters indicate significant differences between different soils at the P<0.05 level.
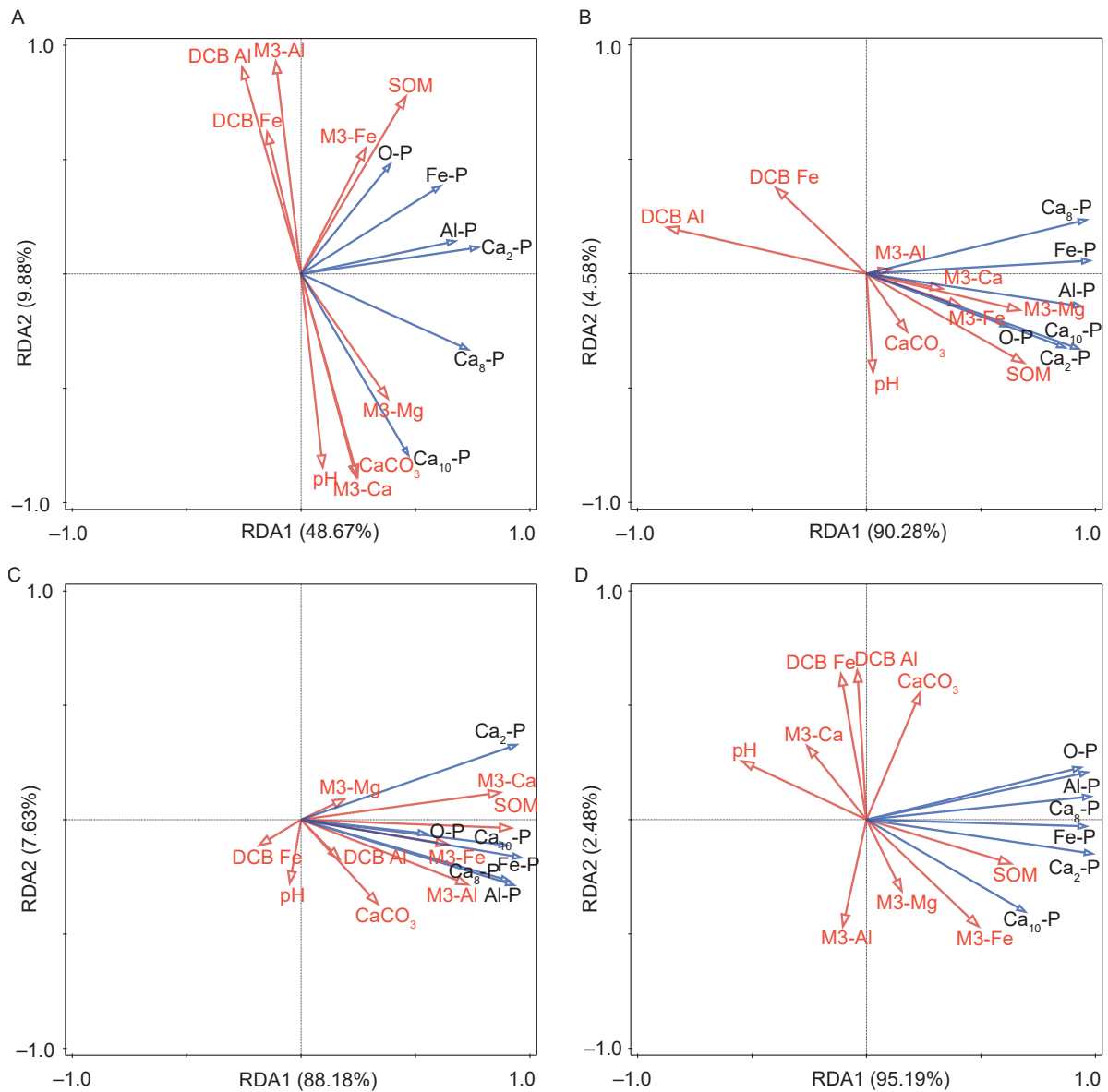
Fig. 3 Redundancy analysis (RDA) between the soil properties and Pi fractions in all soils (A), black soil (B), fluvo-aquic soil (C), and loess soil (D). SOM, soil organic matter; M3-Ca, M3-Mg, M3-Al, and M3-Fe indicate Ca, Mg, Al, and Fe extracted by the Mehlich-3 extraction reagent; DCB Fe, free Fe_2O_3; DCB Al, free Al_2O_3.

3.5. Correlations between soil Pi and SOM

The correlation analysis showed that SOM was positively correlated with most of the Pi fractions (*P*<0.05) (Table 5). Except for O-P, the other Pi fractions had extremely significant positive correlations with SOM in black soil (*P*<0.01), and the slope range was 3.60–6.55 (Table 5). Fluvo-aquic soil was similar to black soil with a slope range of 4.23–19.95 (Table 5). Fe-P, O-P, and Ca_{10}-P were significantly positively correlated with SOM, with a slope range of 0.89–4.73, in loess soil (Table 5). These results indicated that the Pi fractions in fluvo-aquic soil

were the most sensitive to the change in the content of SOM.

4. Discussion

4.1. Responses of Pi fractions in the three soils to different fertilizer practices

The contents of most of the Pi fractions in the three soils increased after long-term P fertilization application (NPK/ NPKS and NPKM) (Table 3). The Pi was divided into the labile-P (Ca_2-P), moderately labile-P (Ca_8-P, Fe-P,

Table 4 Explained percentages of the main contributing factors in redundancy analysis (RDA) ($P<0.05$)

Soil(s)	Factor[1]	Explaination (%)	P-value
All soils	DCB Al	29.4	0.002
	SOM	16.4	0.010
	M3-Fe	6.0	0.038
Black soil	SOM	43.6	0.014
	DCB Al	27.1	0.026
Fluvo-aquic soil	SOM	74.6	0.002
	M3-Fe	10.0	0.012
Loess soil	SOM	38.2	0.022
	M3-Ca	11.3	0.040

[1] DCB Al, free Al_2O_3; SOM, soil organic matter; M3-Fe and M3-Ca indicate Fe and Ca extracted with the Mehlich-3 extraction reagent.

Table 5 Linear correlations between Pi fractions (x) and soil organic matter (y)

Soil type	Pi fraction	Equation	P-value	R^2
Black soil	Ca_2-P	$y=3.6x–74.81$	<0.01	0.88
	Ca_8-P	$y=6.06x–111.92$	<0.01	0.62
	Al-P	$y=5.01x–92.1$	<0.01	0.66
	Fe-P	$y=6.55x–122.64$	<0.01	0.73
	O-P	–	–	–
	Ca_{10}-P	$y=5.33x+23.91$	<0.01	0.62
Fluvo-aquic soil	Ca_2-P	$y=10.72x–104.7$	<0.01	0.82
	Ca_8-P	$y=19.95x–171.43$	<0.01	0.78
	Al-P	$y=4.23x–22.32$	<0.01	0.71
	Fe-P	$y=8.16x–76.25$	<0.01	0.77
	O-P	–	–	–
	Ca_{10}-P	$y=18.7x+64.22$	<0.01	0.84
Loess soil	Ca_2-P	–	–	–
	Ca_8-P	–	–	–
	Al-P	–	–	–
	Fe-P	$y=1.22x+18.02$	<0.05	0.48
	O-P	$y=4.73x+24.76$	<0.05	0.31
	Ca_{10}-P	$y=0.89x+305.51$	<0.01	0.51

and Al-P), and stable P (Ca_{10}-P and O-P) by the Jiang and Gu (1989) Pi fractionation method, and the labile and moderately labile-P could be generated over a short time by P fertilizer application. A previous study reported that stable P was more difficult to form or transform than labile P or moderately labile P in the natural ecosystem (Helfenstein et al. 2018). Similarly, this study showed that the change in stable P could be influenced by P fertilizer application, which greatly increased the contents of Ca_{10}-P and O-P (Table 3), indicating that P fertilization could accelerate the transformation of Pi in cropland soils.

The variation in the Pi fractions in the group of no P application could reflect their availability under P depletion conditions. After depletion for about 10 years, almost all labile-P (Ca_2-P) and moderately labile-P (Ca_8-P, Fe-P, and Al-P) decreased under the CK/NK treatment in the three soils (Table 3), confirming that these Pi fractions

are a potentially available P source for crops. Shen et al. (2019) showed that Ca_8-P is the greatest potential pool for P desorption after Ca_2-P was depleted by sequential extraction using Olsen solution. Gatiboni et al. (2021) demonstrated by path analysis that moderately labile-P showed a high contribution to plant P uptake without P fertilization. We also noticed that some Pi fractions showed changes that were the opposite in the early and late periods under CK/NK treatment, which may be caused by the mineralization of organic P by root residues and the mutual transformations between Pi fractions (De Oliveira et al. 2020). Ca_{10}-P and O-P are generally considered to be relatively stable P, which is difficult for crops to use. We observed that the contents of Ca_{10}-P (in black soil and fluvo-aquic soil) and O-P (in loess soil) were reduced greatly under the CK/NK treatment (Table 3). When the soil was P deficient, almost all of the Pi fractions could be taken up by the crop (De Oliveira et al. 2020). The use of stable P by plants depends on root strategies, such as white lupin forming cluster roots together with their reducing power to allow the destabilization of O-P (Schubert et al. 2020). Our results, in agreement with previous studies (Schubert et al. 2020; Gatiboni et al. 2021), demonstrated that Ca_{10}-P and O-P could also serve as potential sources of P for plants in serious P deficiency.

For the NPK/NPKS treatment, the accumulation of Pi in black soil and fluvo-aquic soil was mainly concentrated in the late stage (2000/2002–2012) (Table 3). Fertilizer application and planting could improve the soil structure and increase the contents of SOM and soil exchangeable Ca (Chen M M et al. 2021), enhancing the transformation of soil minerals and resulting in the formation of poorly crystalline secondary Fe and Al hydroxides (Eriksson et al. 2016), which are conducive to the accumulation of Pi. The accumulation of Pi under NPK/NPKS in loess soil mainly occurred in the early stage (1990–2000) (Table 3), possibly because of the lower rainfall occurrence than in black soil and fluvo-aquic soil (Shen et al. 2014; Helfenstein et al. 2018), although more specific reasons need to be further investigated.

The Pi accumulation had higher contents in most stages (>200 mg kg^{-1}) under NPKM in the three soils (Table 3). The P of manure mainly existed in the form of Pi (Wu et al. 2017), and a large amount of Pi input (from chemical P fertilizer or manure) was the main reason for the Pi accumulation in each fraction (Table 3).

4.2. Effects of soil properties on Pi fractions

In this study, Ca_{10}-P had the highest proportion of 33.5–48.8% among the Pi fractions in the three soils (Fig. 1). $CaCO_3$ was abundant in each test soil ($CaCO_3$>20 g kg^{-1})

(Fig. 2), and it could dissolve to form Ca^{2+} causing the precipitation of Ca-P complex (Weihrauch and Opp 2018). The content of this precipitate was positively correlated with the content of Ca^{2+} and pH (Tunesi et al. 1999; Ma et al. 2019). It was found that the $CaCO_3$ and M3-Ca contents and pH were the lowest in black soil (Fig. 2), so the Ca_{10}-P content and proportion in black soil were lower than in fluvo-aquic soil and loess soil (Fig. 1). Another piece of evidence shows that the change in Ca_8-P was the greatest among the Pi fractions under different P application rates (Fig. 1; Tables 1 and 3), suggesting that Ca^{2+} or some calcareous material was the main determinant of the Pi fractions in the test soils.

The contribution of SOM to the variation in the Pi fractions reached a significant level ($P<0.05$) in all three non-acidic soils (Fig. 3; Table 4). The increase in SOM decreased the P bonding energy and maximum buffering capacity (Yang et al. 2019), suggesting that a higher content of SOM improves the soil's ability to retain labile and moderately labile P. This was consistent with our findings, in which the total proportion of labile and moderately labile P was higher in black soil (48.8%) than fluvo-aquic soil (28.6%) or loess soil (27.4%) (Fig. 1). For individual soils, SOM mainly explained the variation in soil Pi (Fig. 3-B–D; Table 4), which was similar to previous research indicating that SOM was a significant predictor of the P forms in soils (Chen S et al. 2021). On the one hand, SOM is usually associated with Fe and Al hydroxides, which form organic–inorganic composites or poorly crystalline Fe and Al hydroxides and enhance the formation of Fe-P and Al-P (Eriksson et al. 2016; Wang Z C et al. 2019; Bao et al. 2021). SOM, Ca, and P can form terpolymer complexes, and SOM can also adsorb P via a Ca^{2+} bridge (Audette et al. 2020; Li F Y et al. 2021), which inhibits the transformation of amorphous calcium phosphate into phases that are thermodynamically more stable (Ge et al. 2020). Our results showed that SOM was significantly ($P<0.01$) correlated with Ca_2-P, Ca_8-P, Al-P, and Fe-P in black soil and fluvo-aquic soil (Table 5), indicating that SOM plays an important role in improving the availability of soil P.

Redundancy analysis showed that DCB Al and M3-Fe in black soil, DCB Al in fluvo-aquic soil, and M3-Ca in loess soil significantly ($P<0.05$) explained the variation in the Pi fractions (Fig. 3; Table 4). These metals extracted with chemical reagents are usually poorly crystalline or amorphous compounds in soil and play an important role in P adsorption (Mehra and Jackson 1960; Mehlich 1984; Liu and Hesterberg 2011; Wang X et al. 2019; Lin et al. 2020). In the soil, these metals likely interact with SOM to form P-SOM-metal complexes, maintaining the higher availability of P (Wang et al. 2016; Ge et al. 2020; Li et al. 2020). Black soil had the highest contents of SOM, DCB Fe, DCB Al, M3-Fe, and M3-Al (Fig. 2), and accordingly, the proportions of Fe-P and Al-P were the highest among the three soils (Fig. 1). These results suggested that the dominant properties of soil determined the distribution of Pi fractions, and more interactions among the soil properties seemed to influence the retention and transformation of the Pi fractions.

5. Conclusion

The content of Ca_{10}-P was the highest among the Pi fractions in the three non-acidic soils. P depletion was the most direct way to verify the availability of the Pi fractions, which indicated that Ca_{10}-P was easy to utilize in black soil and fluvo-aquic soil, whereas O-P was easy to utilize in loess soil. P application accelerated the transformation of P in soil, resulting in the accumulation of different Pi fractions. However, different soil types and fertilization practices caused Pi accumulation with differences in timing and the fractions. Black soil had higher SOM and Fe and Al oxides compared with fluvo-aquic soil and loess soil. Their interactions allowed more of the labile and moderately labile Pi to be retained. Considering that manure could increase SOM, we suggest that the combined application of mineral fertilizer and manure is a way to rapidly increase the soil P level, but the P accumulation rate and the availability of various Pi fractions should be considered.

Acknowledgements

Declaration of competing interest

The authors declare that they have no conflict of interest.

References

Andersson K O, Tighe M K, Guppy C N, Milham P J, McLaren T I. 2015. Incremental acidification reveals phosphorus release dynamics in alkaline vertic soils. Geoderma, 259, 35–44.

Audette Y, Smith D S, Parsons C T, Chen W B, Rezanezhad F, Van Cappellen P. 2020. Phosphorus binding to soil organic matter via ternary complexes with calcium. Chemosphere, 260, 127624.

Bao Y P, Bolan N S, Lai J H, Wang Y S, Jin X H, Kirkham M B, Wu X L, Fang Z, Zhang Y, Wang H L. 2021. Interactions between organic matter and Fe (hydr)oxides and their influences on immobilization and remobilization of metal(loid)s: A review. *Critical Reviews in Environmental Science and Technology*, **9**, 1–22.

Chen M M, Zhang S R, Liu L, Wu L P, Ding X D. 2021. Combined organic amendments and mineral fertilizer application increase rice yield by improving soil structure, P availability and root growth in saline-alkaline soil. *Soil and Tillage Research*, **212**, 105060.

Chen M P, Graedel T E. 2016. A half-century of global phosphorus flows, stocks, production, consumption, recycling, and environmental impacts. *Global Environmental Change*, **36**, 139–152.

Chen S, Cade-Menun B J, Bainard L D, St Luce M, Hu Y F, Chen Q. 2021. The influence of long-term N and P fertilization on soil P forms and cycling in a wheat/fallow cropping system. *Geoderma*, **404**, 115274.

Cooper J, Lombardi R, Boardman D, Carliell-Marquet C. 2011. The future distribution and production of global phosphate rock reserves. *Resources Conservation and Recycling*, **57**, 78–86.

Deiss L, de Moraes A, Maire V. 2018. Environmental drivers of soil phosphorus composition in natural ecosystems. *Biogeosciences*, **15**, 4575–4592.

Eriksson A K, Gustafsson J P, Hesterberg D. 2015. Phosphorus speciation of clay fractions from long-term fertility experiments in Sweden. *Geoderma*, **241**, 68–74.

Eriksson A K, Hillier S, Hesterberg D, Klysubun W, Ulen B, Gustafsson J P. 2016. Evolution of phosphorus speciation with depth in an agricultural soil profile. *Geoderma*, **280**, 29–37.

Fink J R, Inda A V, Tiecher T, Barron V. 2016. Iron oxides and organic matter on soil phosphorus availability. *Ciencia e Agrotecnologia*, **40**, 369–379.

Gatiboni L C, Schmitt D E, Tiecher T, Veloso M G, dos Santos D R, Kaminski J, Brunetto G. 2021. Plant uptake of legacy phosphorus from soils without P fertilization. *Nutrient Cycling in Agroecosystems*, **119**, 139–151.

Ge X F, Wang L J, Zhang W J, Putnis C V. 2020. Molecular understanding of humic acid-limited phosphate precipitation and transformation. *Environmental Science and Technology*, **54**, 207–215.

Hansen J C, Cade-Menun B J, Strawn D G. 2004. Phosphorus speciation in manure-amended alkaline soils. *Journal of Environmental Quality*, **33**, 1521–1527.

Helfenstein J, Tamburini F, von Sperber C, Massey M S, Pistocchi C, Chadwick O A, Vitousek P M, Kretzschmar R, Frossard E. 2018. Combining spectroscopic and isotopic techniques gives a dynamic view of phosphorus cycling in soil. *Nature Communications*, **9**, 3226.

Jiang B F, Gu Y C. 1989. A suggested fractionation scheme of inorganic phosphorus in calcareous soils. *Scientia Agricultura Sinica*, **22**, 58–66. (in Chinese)

Jiao X Q, Lyu Y, Wu X B, Li H G, Cheng L Y, Zhang C C, Yuan L X, Jiang R F, Jiang B W, Rengel Z, Zhang F S, Davies W J, Shen J B. 2016. Grain production versus resource and environmental costs: towards increasing sustainability of nutrient use in China. *Journal of Experimental Botany*, **67**, 4935–4949.

Khan A, Lu G Y, Ayaz M, Zhang H T, Wang R J, Lv F L, Yang X Y, Sun B H, Zhang S L. 2018. Phosphorus efficiency, soil phosphorus dynamics and critical phosphorus level under long-term fertilization for single and double cropping systems. *Agriculture Ecosystems and Environment*, **256**, 1–11.

Khosravi A, Zarei M, Ronaghi A. 2017. Influence of biofertilizers and phosphate sources on the phosphorus uptake of lettuce and chemical forms of phosphorus in soil. *Communications in Soil Science and Plant Analysis*, **48**, 2701–2714.

Li F Y, Zhang Q, Klumpp E, Bol R, Nischwitz V, Ge Z, Liang X Q. 2021. Organic carbon linkage with soil colloidal phosphorus at regional and field scales: Insights from size fractionation of fine particles. *Environmental Science and Technology*, **55**, 5815–5825.

Li H, Huang G, Meng Q, Ma L, Yuan L, Wang F, Zhang W, Cui Z, Shen J, Chen X, Jiang R, Zhang F. 2011. Integrated soil and plant phosphorus management for crop and environment in China. A review. *Plant and Soil*, **349**, 157–167.

Li J Q, Nie M, Pendall E. 2020. Soil physico-chemical properties are more important than microbial diversity and enzyme activity in controlling carbon and nitrogen stocks near Sydney, Australia. *Geoderma*, **366**, 114201.

Lin J W, Zhao Y Y, Zhan Y H, Wang Y. 2020. Influence of coexisting calcium and magnesium ions on phosphate adsorption onto hydrous iron oxide. *Environmental Science and Pollution Research*, **27**, 11303–11319.

Liu J, Han C Q, Zhao Y H, Yang J J, Cade-Menun B J, Hu Y F, Li J M, Liu H, Sui P, Chen Y Q, Ma Y B. 2020. The chemical nature of soil phosphorus in response to long-term fertilization practices: Implications for sustainable phosphorus management. *Journal of Cleaner Production*, **272**, 123093.

Liu J, Yang J J, Cade-Menun B J, Hu Y F, Li J M, Peng C, Ma Y B. 2017. Molecular speciation and transformation of soil legacy phosphorus with and without long-term phosphorus fertilization: Insights from bulk and microprobe spectroscopy. *Scientific Reports*, **7**, 15354.

Liu Y T, Hesterberg D. 2011. Phosphate bonding on noncrystalline Al/Fe-hydroxide coprecipitates. *Environmental Science and Technology*, **45**, 6283–6289.

Lu R K. 1999. *Soil and Agro-Chemistry Analytical Method*. China Agricultural Science and Technology Press, Beijing. (in Chinese)

Ma J, Ma Y L, Wei R F, Chen Y L, Weng L P, Ouyang X X, Li Y T. 2021. Phosphorus transport in different soil types and the contribution of control factors to phosphorus retardation. *Chemosphere*, **276**, 130012.

Ma Y L, Ma J, Peng H, Weng L P, Chen Y L, Li Y T. 2019. Effects of iron, calcium, and organic matter on phosphorus behavior in fluvo-aquic soil: Farmland investigation and

aging experiments. *Journal of Soils and Sediments*, **19**, 3994–4004.

MacDonald G K, Bennett E M, Potter P A, Ramankutty N. 2011. Agronomic phosphorus imbalances across the world's croplands. *Proceedings of the National Academy of Sciences of the United States of America*, **108**, 3086–3091.

Mehlich A. 1984. Mehlich 3 soil test extractant: A modification of Mehlich 2 extractant. *Communications in Soil Science and Plant Analysis*, **15**, 1409–1416.

Mehra O P, Jackson M L. 1960. Iron oxides removal from soil and clays by a dithionite-citrate system buffered with sodium bicarbonate. *Clays and Clay Minerals*, **7**, 317–327.

Meyer G, Bell M J, Lombi E, Doolette C L, Brunetti G, Novotny E H, Klysubun W, Zhang Y Q, Kopittke P M. 2021. Phosphorus speciation in the fertosphere of highly concentrated fertilizer bands. *Geoderma*, **403**, 115208.

Murphy J, Riley J P. 1962. A modified single solution method for the determination of phosphate in natural waters. *Analytica Chimica Acta*, **27**, 31–36.

De Oliveira L E Z, Nunes R D, de Sousa D M G, de Figueiredo C C. 2020. Dynamics of residual phosphorus forms under different tillage systems in a Brazilian Oxisol. *Geoderma*, **367**, 114254.

Pizzeghello D, Berti A, Nardi S, Morari F. 2011. Phosphorus forms and P-sorption properties in three alkaline soils after long-term mineral and manure applications in north-eastern Italy. *Agriculture Ecosystems and Environment*, **141**, 58–66.

Sato S, Solomon D, Hyland C, Ketterings Q M, Lehmann J. 2005. Phosphorus speciation in manure and manure-amended soils using XANES spectroscopy. *Environmental Science and Technology*, **39**, 7485–7491.

Schmieder F, Bergstrom L, Riddle M, Gustafsson J P, Klysubun W, Zehetner F, Condron L, Kirchmann H. 2018. Phosphorus speciation in a long-term manure-amended soil profile — Evidence from wet chemical extraction, ^{31}P-NMR and P K-edge XANES spectroscopy. *Geoderma*, **322**, 19–27.

Schubert S, Steffens D, Ashraf I. 2020. Is occluded phosphate plant-available? *Journal of Plant Nutrition and Soil Science*, **183**, 338–344.

Shen P, Xu M, Zhang H, Yang X, Huang S, Zhang S, He X. 2014. Long-term response of soil Olsen P and organic C to the depletion or addition of chemical and organic fertilizers. *Catena*, **118**, 20–27.

Shen Y, Duan Y H, McLaughlin N, Huang S M, Guo D D, Xu M H. 2019. Phosphorus desorption from calcareous soils with different initial Olsen-P levels and relation to phosphate fractions. *Journal of Soils and Sediments*, **19**, 2997–3007.

Tunesi S, Poggi V, Gessa C. 1999. Phosphate adsorption and precipitation in calcareous soils: the role of calcium ions in solution and carbonate minerals. *Nutrient Cycling in Agroecosystems*, **53**, 219–227.

Wang H, Zhu J, Fu Q L, Hong C, Hu H Q, Violante A. 2016. Phosphate adsorption on uncoated and humic acid-coated iron oxides. *Journal of Soils and Sediments*, **16**, 1911–1920.

Wang X, Phillips B L, Boily J F, Hu Y, Hu Z, Yang P, Feng X, Xu W, Zhu M. 2019. Phosphate sorption speciation and precipitation mechanisms on amorphous aluminum hydroxide. *Soil Systems*, **3**, 20.

Wang Y, Bauke S L, von Sperber C, Tamburini F, Guigue J, Winkler P, Kaiser K, Honermeier B, Amelung W. 2021. Soil phosphorus cycling is modified by carbon and nitrogen fertilization in a long-term field experiment. *Journal of Plant Nutrition and Soil Science*, **184**, 282–293.

Wang Z C, Huang S, Li D H. 2019. Decomposition of cyanobacterial bloom contributes to the formation and distribution of iron-bound phosphorus (Fe-P): Insight for cycling mechanism of internal phosphorus loading. *Science of the Total Environment*, **652**, 696–708.

Weihrauch C, Opp C. 2018. Ecologically relevant phosphorus pools in soils and their dynamics: The story so far. *Geoderma*, **325**, 183–194.

Wu Q H, Zhang S X, Zhu P, Huang S M, Wang B R, Zhao L P, Xu M G. 2017. Characterizing differences in the phosphorus activation coefficient of three typical cropland soils and the influencing factors under long-term fertilization. *PLoS ONE*, **12**, e0176437.

Yadav B K, Verma A. 2012. Phosphate solubilization and mobilization in soil through microorganisms under arid ecosystems. *The Functioning of Ecosystems*, **27**, 93–108.

Yamamoto K, Hashimoto Y, Kang J, Kobayashi K. 2018. Speciation of phosphorus zinc and copper in soil and water dispersible colloid affected by a long-term application of swine manure compost. *Environmental Science and Technology*, **52**, 13270–13278.

Yan Z J, Chen S, Dari B, Sihi D, Chen Q. 2018. Phosphorus transformation response to soil properties changes induced by manure application in a calcareous soil. *Geoderma*, **322**, 163–171.

Yang X Y, Chen X W, Yang X T. 2019. Effect of organic matter on phosphorus adsorption and desorption in a black soil from Northeast China. *Soil and Tillage Research*, **187**, 85–91.

Zhang H Z, Shi L L, Lu H B, Shao Y H, Liu S R, Fu S L. 2020. Drought promotes soil phosphorus transformation and reduces phosphorus bioavailability in a temperate forest. *Science of the Total Environment*, **732**, 139295.

Zhu J, Li M, Whelan M. 2018. Phosphorus activators contribute to legacy phosphorus availability in agricultural soils: A review. *Science of the Total Environment*, **612**, 522–537.